

Synthesis, Crystal Structures, and Fluxional Behavior of Donor-Bridged Bis(silylene)molybdenum and -chromium Complexes

Keiji Ueno,* Akira Masuko, and Hiroshi Ogino*

Department of Chemistry, Graduate School of Science, Tohoku University,
Aoba-ku, Sendai 980-8578, Japan

Received March 22, 1999

Donor-bridged bis(silylene)molybdenum and -chromium complexes $\text{CpM}(\text{CO})_2\{(\text{SiMe}_2)\cdots\text{Do}\cdots(\text{SiMe}_2)\}$ ($\text{Cp} = \eta\text{-C}_5\text{H}_5$; $\text{M} = \text{Mo}$, $\text{Do} = \text{OMe}$ (**1a**); $\text{M} = \text{Mo}$, $\text{Do} = \text{NEt}_2$ (**1b**); $\text{M} = \text{Cr}$, $\text{Do} = \text{OMe}$ (**2**)) were synthesized by photolysis of a C_6D_6 solution containing $\text{CpM}(\text{CO})_3\text{Me}$ and $\text{HSiMe}_2\text{SiMe}_2\text{Do}$. The X-ray crystal structures of **1a**, **1b**, and **2** revealed that the $\text{M}\text{-Si}$ bonds (2.4795(9) and 2.4804(9) Å for **1a**, 2.4996(9) and 2.5008(9) Å for **1b**, and 2.355(2) Å for **2**) are significantly shorter than those of structurally similar silylmolybdenum and -chromium complexes, while the $\text{Si}\text{-O}$ bonds in **1a** (1.782(2) and 1.788(3) Å) and **2** (1.788(3) Å) and the $\text{Si}\text{-N}$ bonds in **1b** (1.933(2) and 1.923(3) Å) are much longer than usual $\text{Si}\text{-O}$ and $\text{Si}\text{-N}$ single bonds. These structural data indicate that the $\text{M}\text{-Si}$ bonds bear partial double-bond character, whereas the $\text{Si}\text{-O}$ and $\text{Si}\text{-N}$ bonds are regarded as a hybrid of covalent bonding and dative bonding. The unsaturated nature of the metal-silicon bonds is also shown by the significant downfield shift of the ^{29}Si NMR signals (**1a**, $\delta = 117.6$ ppm; **1b**, $\delta = 80.5$ ppm; **2**, $\delta = 128.6$ ppm) compared to those of structurally similar silylmolybdenum and -chromium complexes. Complexes **1a**, **1b**, and **2** showed fluxional behavior due to silylene-methyl group exchange and, in the case of **1b**, $\text{N}\text{-Et}$ group exchange. A mechanism involving the generation of a base-free silyl(silylene) complex as the key intermediate is proposed to explain the fluxional process.

Introduction

Considerable attention has been focused on the synthesis and chemical behavior of silylene-transition metal complexes.^{1–5} Silyl(silylene) transition metal complexes $\text{L}_m\text{M}(\text{SiR}_2)\text{SiR}_3$ are attractive synthetic targets since such complexes have been assumed to be key intermediates in metal-catalyzed substituent scrambling and skeletal redistribution of organosilicon and organosilicon-transition metal compounds.^{5–12} Pan-

nell,^{6,13} the present authors,^{7,14} and Turner¹⁵ reported convincing evidence for the formation of silyl(silylene)-iron intermediates during the degradation of oligosilanyliron complexes. Silyl(silylene) complexes have been isolated as intramolecular^{14,16–19} or external²⁰ donor-stabilized silyl(silylene) complexes. A unique type of the intramolecular donor-stabilized complexes is the “donor-bridged bis(silylene) complex” **A** (Scheme 1), which is equivalent to a resonance hybrid of two canonical forms

(1) Tilley, T. D. In *The Chemistry of Organic Silicon Compounds*; Patai, S., Rappoport, Z., Eds.; John Wiley & Sons: New York, 1989; Chapter 24, p 1415.

(2) (a) Zybilla, C. *Top. Curr. Chem.* **1991**, *160*, 1. (b) Zybilla, C.; Handwerker, H.; Friedrich, H. *Adv. Organomet. Chem.* **1994**, *36*, 229.

(3) Lickiss, P. D. *Chem. Soc. Rev.* **1992**, 271.

(4) Eisen, M. S. In *The Chemistry of Organic Silicon Compounds, Volume 2*; Rappoport, Z., Apeloig, Y., Eds.; John Wiley & Sons: New York, 1998; Chapter 35, p 2037.

(5) Shama, H. K.; Pannell, K. H. *Chem. Rev.* **1995**, *95*, 1351.

(6) (a) Pannell, K. H.; Cervantes, J.; Hernandez, C.; Cassias, J.; Vincenti, S. *Organometallics* **1986**, *5*, 1056. (b) Pannell, K. H.; Rozell, J. M., Jr.; Hernandez, C. *J. Am. Chem. Soc.* **1989**, *111*, 4482. (c) Pannell, K. H.; Wang, L.-J.; Rozell, J. M. *Organometallics* **1989**, *8*, 550. (d) Pannell, K. H.; Rozell, J. M., Jr.; Vincenti, S. *Adv. Chem. Ser.* **1990**, *224*, 329. (e) Pannell, K. H.; Sharma, H. *Organometallics* **1991**, *10*, 954. (f) Hernandez, C.; Sharma, H. K.; Pannell, K. H. *J. Organomet. Chem.* **1993**, *462*, 259. (g) Jones, K. L.; Pannell, K. H. *J. Am. Chem. Soc.* **1993**, *115*, 11336. (h) Pannell, K. H.; Brun, M.-C.; Sharma, H.; Jones, K.; Sharma, S. *Organometallics* **1994**, *13*, 1075. (i) Zhang, Z.; Sanchez, R.; Pannell, K. H. *Organometallics* **1995**, *14*, 2605.

(7) (a) Tobita, H.; Ueno, K.; Ogino, H. *Chem. Lett.* **1986**, 1777. (b) Tobita, H.; Ueno, K.; Ogino, H. *Bull. Chem. Soc. Jpn.* **1988**, *61*, 2797. (c) Ueno, K.; Tobita, H.; Ogino, H. *Chem. Lett.* **1990**, 369. (d) Ueno, K.; Hamashima, N.; Shimoi, M.; Ogino, H. *Organometallics* **1991**, *10*, 959.

(8) Hashimoto, H.; Tobita, H.; Ogino, H. *J. Organomet. Chem.* **1995**, *499*, 205.

(9) Pestana, D. C.; Koloski, T. S.; Berry, D. H. *Organometallics* **1994**, *13*, 4173.

(10) Mitchell, G. P.; Tilley, T. D.; Yap, G. P. A.; Rheingold, A. L. *Organometallics* **1995**, *14*, 5472.

(11) Tanaka, Y.; Yamashita, H.; Tanaka, M. *Organometallics* **1995**, *14*, 530.

(12) Tamao, K.; Sun, G.-R.; Kawachi, A. *J. Am. Chem. Soc.* **1995**, *117*, 8043.

(13) Pannell, K. H.; Sharma, H. K.; Kapoor, R. N.; Cervantes-Lee, F. *J. Am. Chem. Soc.* **1997**, *119*, 9315.

(14) (a) Ueno, K.; Tobita, H.; Shimoi, M.; Ogino, H. *J. Am. Chem. Soc.* **1988**, *110*, 4092. (b) Tobita, H.; Ueno, K.; Shimoi, M.; Ogino, H. *J. Am. Chem. Soc.* **1990**, *112*, 3415. (c) Ueno, K.; Ito, S.; Endo, K.; Tobita, H.; Inomata, S.; Ogino, H. *Organometallics* **1994**, *13*, 3309.

(15) Haynes, A.; George, M. W.; Haward, M. T.; Poliakov, M.; Turner, J. J.; Boag, N. M.; Green, M. *J. Am. Chem. Soc.* **1991**, *113*, 2011.

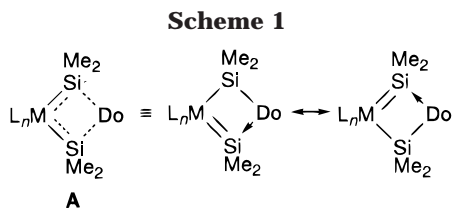
(16) (a) Takeuchi, T.; Tobita, H.; Ogino, H. *Organometallics* **1991**, *10*, 835. (b) Tobita, H.; Wada, H.; Ueno, K.; Ogino, H. *Organometallics* **1994**, *13*, 2545. (c) Okazaki, M.; Tobita, H.; Ogino, H. *Chem. Lett.* **1997**, 437. (d) Tobita, H.; Kurita, H.; Ogino, H. *Organometallics* **1998**, *17*, 2850. (e) Tobita, H.; Kurita, H.; Ogino, H. *Organometallics* **1998**, *17*, 2844.

(17) Ueno, K.; Masuko, A.; Ogino, H. *Organometallics* **1997**, *16*, 5023.

(18) Wada, H.; Tobita, H.; Ogino, H. *Chem. Lett.* **1998**, 993.

(19) Nlate, S.; Herdtweck, E.; Fischer, R. A. *Angew. Chem., Int. Ed. Engl.* **1996**, *35*, 1861.

(20) (a) Ueno, K.; Nakano, K.; Ogino, H. *Chem. Lett.* **1996**, 459. (b) Ueno, K.; Sakai, M.; Ogino, H. *Organometallics* **1998**, *17*, 2138.



of intramolecular donor-stabilized silyl(silylene) complexes and thus has two unsaturated silicon atoms in the molecule.^{14,16–18} The first donor-free silyl(silylene) complex was recently synthesized by the reaction of thermally stable silylene with a platinum complex.²¹

In the previous paper, we reported the synthesis of donor-bridged bis(silylene)tungsten complexes, CpW(CO)₂{(SiMe₂)[⋯]Do[⋯](SiMe₂)} (Cp = η-C₅H₅; Do = OMe (**3a**), NEt₂ (**3b**)), by photolysis of CpW(CO)₃Me in the presence of a hydrodisilane HSiMe₂SiMe₂Do.¹⁷ In this paper, we report the synthesis and crystal structures of the lighter congeners of the donor-bridged bis(silylene)tungsten complexes CpM(CO)₂{(SiMe₂)[⋯]Do[⋯](SiMe₂)} (**1a**, M = Mo, Do = OMe; **1b**, M = Mo, Do = NEt₂; **2**, M = Cr, Do = OMe), which complete the series of bis(silylene) complexes of the group 6 metals. To our knowledge, there has been only one example of an isolated molybdenum complex with a silylene ligand,²² and **1a** and **1b** are the first structurally determined silylenemolybdenum complexes. The bis(silylene)tungsten complexes showed fluxional behavior due to the rotation of the silylene ligand around the tungsten–silylene bond.¹⁷ Similar fluxional behavior has been observed for germylene rotation in silylene(germylene) and bis(germylene)iron complexes²³ and, very recently, for silylene rotation in bis(silylene)ruthenium complexes.¹⁸ The bis(silylene)molybdenum and -chromium complexes, **1a**, **1b**, and **2**, show fluxional behavior due to the rotation of the silylene ligand similar to that observed for the bis(silylene)tungsten complexes.

Experimental Section

All manipulations were performed either using standard Schlenk tube techniques under a nitrogen atmosphere, using vacuum line techniques, or in a drybox under a nitrogen atmosphere. Toluene was dried and deoxygenated by refluxing over sodium benzophenone ketyl followed by distillation under a nitrogen atmosphere. Benzene-*d*₆ and toluene-*d*₆ were dried over a potassium mirror and distilled directly into the reaction vessel before use. CpMo(CO)₃Me²⁴ and CpCr(CO)₃Me²⁵ were prepared according to the literature methods. Syntheses of HSiMe₂SiMe₂NET₂ and HSiMe₂SiMe₂OMe were described in our previous paper.¹⁷ Nuclear magnetic resonance (NMR) spectra were recorded on a Bruker ARX-300 Fourier transform spectrometer. Infrared (IR) spectra were obtained on a HORIBA FT-200 spectrometer. Mass spectra were recorded on a JEOL HX-110 spectrometer at the Instrumental Analysis Center for Chemistry, Tohoku University. Elemental analyses were also performed at the Instrumental Analysis Center for Chemistry, Tohoku University.

(21) Gehrhus, B.; Hitchcock, P. B.; Lappert, M. F.; Maciejewski, H. *Organometallics* **1998**, *17*, 5599.

(22) Chauhan, B. P. S.; Corriu, R. J. P.; Lanneau, G. F.; Priou, C. *Organometallics* **1995**, *14*, 1657.

(23) (a) Koe, J. R.; Tobita, H.; Suzuki, T.; Ogino, H. *Organometallics* **1992**, *11*, 150. (b) Koe, J. R.; Tobita, H.; Ogino, H. *Organometallics* **1992**, *11*, 2479.

(24) Fischer, E. O. *Inorg. Synth.* **1963**, *7*, 136.

(25) Alt, H. G. *J. Organomet. Chem.* **1977**, *124*, 167.

Synthesis of Cp(OC)₂Mo{(SiMe₂)[⋯]OMe[⋯](SiMe₂)} (1a**).** A Pyrex sample tube (10 mm o.d., 8 mm i.d.) with a ground-glass joint was charged with CpMo(CO)₃Me (0.70 g, 2.7 mmol) and HSiMe₂SiMe₂OMe (0.59 g, 4.0 mmol) and connected to a vacuum line via a ground-glass joint. Toluene (about 5 mL) was transferred to the sample tube by conventional trap-to-trap distillation. The sample tube was then flame-sealed under vacuum. The solution was irradiated for 90 min externally with a medium-pressure Hg arc lamp (Ushio UV-450) placed in a water-cooled quartz jacket. The sample tube was immersed in ice–water during the irradiation. The distance from the light source to the sample was ca. 4 cm. After irradiation, the reaction mixture was transferred into a Schlenk tube, concentrated, and cooled to –18 °C in a refrigerator to give air- and moisture-sensitive yellow crystals of **1a** (0.32 g, 0.88 mmol, 33%). ¹H NMR (300 MHz, C₆D₆, 295 K): δ 4.77 (s, 5H, C₅H₅), 2.62 (s, 3H, OCH₃), 0.47 (br, 6H, SiCH₃), 0.44 (br, 6H, SiCH₃). ¹³C NMR (75.5 MHz, C₆D₆, 295 K): δ 237.0 (CO), 88.0 (C₅H₅), 51.9 (OCH₃), 9.2 (br, SiCH₃), 6.5 (br, SiCH₃). ²⁹Si NMR (59.6 MHz, C₆D₆, DEPT, 295 K): δ 117.6. IR (C₆D₆): ν_{CO} 1915, 1848 cm⁻¹. MS (EI, 70 eV): *m/z* 366 (M⁺, 100.0), 306 (M⁺ – 4CH₃, 82.8). Anal. Calcd for C₁₂H₂₀MoO₃Si₂: C, 39.55; H, 5.53. Found: C, 39.79; H, 5.24.

Synthesis of Cp(OC)₂Mo{(SiMe₂)[⋯]NET₂[⋯](SiMe₂)} (1b**).** Complex **1b** was synthesized and isolated in 44% yield in a manner similar to that of **1a** using CpMo(CO)₃Me (0.42 g, 1.7 mmol) and HSiMe₂SiMe₂NET₂ (0.77 g, 4.1 mmol). ¹H NMR (300 MHz, C₆D₆, 295 K): δ 4.84 (s, 5H, C₅H₅), 2.40 (br, 4H, *J* = 7.0 Hz, NCH₂CH₃), 0.67 (br, 6H, SiCH₃), 0.51 (t, 6H, *J* = 7.0 Hz, NCH₂CH₃), 0.35 (br, 6H, SiCH₃). ¹³C NMR (75.5 MHz, C₆D₆, 295 K): δ 237.4 (CO), 88.0 (C₅H₅), 40.7 (br, NCH₂CH₃), 38.7 (br, NCH₂CH₃), 10.4 (NCH₂CH₃), 10.1 (br, SiCH₃), 6.3 (br, SiCH₃). ²⁹Si NMR (59.6 MHz, C₆D₆, DEPT, 295 K): δ 80.5. IR (C₆D₆): ν_{CO} 1903, 1834 cm⁻¹. MS (EI, 70 eV): *m/z* 407 (M⁺, 100.0), 347 (M⁺ – 4CH₃ – 2H, 26.3), 130 (M⁺ – CpMo(CO), 92.7). Anal. Calcd for C₁₅H₂₇MoNO₂Si₂: C, 44.43; H, 6.71; N, 3.45. Found: C, 44.69; H, 6.96; N, 3.52.

Synthesis of Cp(OC)₂Cr{(SiMe₂)[⋯]OMe[⋯](SiMe₂)} (2**).** Complex **2** was synthesized and isolated in a manner similar to that of **1a** by the photolysis of CpCr(CO)₃Me (0.18 g, 0.80 mmol) and HSiMe₂SiMe₂OMe (0.18 g, 1.2 mmol) for 15 min (12% yield). ¹H NMR (300 MHz, C₆D₆, 295 K): δ 4.21 (s, 5H, C₅H₅), 2.56 (s, 3H, OCH₃), 0.59 (br, 6H, SiCH₃), 0.19 (br, 6H, SiCH₃). ¹³C NMR (75.5 MHz, C₆D₆, 295 K): δ 243.7 (CO), 84.0 (C₅H₅), 52.3 (OCH₃), 8.1 (br, SiCH₃), 6.4 (br, SiCH₃). ²⁹Si NMR (59.6 MHz, C₆D₆, DEPT, 295 K): δ 128.6. IR (C₆D₆): ν_{CO} 1900, 1838 cm⁻¹. MS (EI, 70 eV): *m/z* 320 (M⁺, 100.0), 264 (M⁺ – 2CO, 85.2). Anal. Calcd for C₁₂H₂₀CrO₃Si₂: C, 44.98; H, 6.29. Found: C, 44.81; H, 6.28.

X-ray Crystal Structure Determination of **1a, **1b**, and **2**.** A single crystal of **1a**, **1b**, or **2** was sealed in a glass capillary under an atmosphere of dry nitrogen. Intensity data for X-ray crystal structure analysis were collected on a RIGAKU AFC-6S four-circle diffractometer with graphite-monochromated Mo Kα radiation at 293 K. No absorption correction was applied. Space group was determined based on the systematic absences and the subsequent least-squares refinement. For **2**, the centrosymmetric space group *Pnma* was adopted since the *E*-statistics supported the centrosymmetric space group and the solution by the acentrosymmetric alternative *Pn2₁a* was found to be computationally unstable. Crystallographic data for **1a**, **1b**, and **2** are summarized in Table 1. The structures were solved by Patterson and Fourier transform methods (SHELXS-86).²⁶ All non-hydrogen atoms were refined by full-matrix least-squares techniques with anisotropic displacement parameters (SHELXL-93).²⁷ All hydrogen atoms were placed at their geometrically calculated positions (*d*_{CH} = 0.98 Å for

(26) Sheldrick, G. M. *SHELXS-86, Program for Crystal Structure Determination*; University of Göttingen: Göttingen, Germany, 1986.

(27) Sheldrick, G. M. *SHELXL-93, Program for Crystal Structure Determination*; University of Göttingen: Göttingen, Germany, 1993.

Table 1. Crystal Data and Structure Refinement for **1a**, **1b**, and **2**

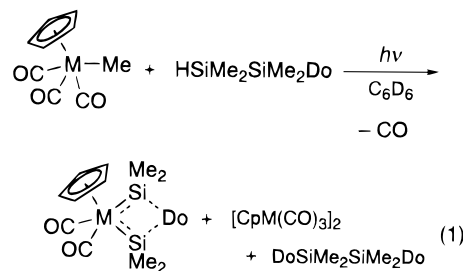
	1a	1b	2
empirical formula	C ₁₂ H ₂₀ MoO ₃ Si ₂	C ₁₅ H ₂₇ MoNO ₂ Si ₂	C ₁₂ H ₂₀ CrO ₃ Si
fw	364.40	405.50	320.46
cryst syst	monoclinic	monoclinic	orthorhombic
space group	<i>P</i> 2 ₁ / <i>n</i>	<i>P</i> 2 ₁ / <i>a</i>	<i>Pnma</i>
unit cell dimens			
<i>a</i> /Å	15.0938(13)	16.667(2)	12.900(2)
<i>b</i> /Å	12.0680(9)	8.8103(7)	14.456(2)
<i>c</i> /Å	9.0823(7)	12.9121(12)	8.5349(8)
β/deg	95.89(2)	94.59(2)	
volume/Å ³	1645.6(2)	1889.9(3)	1591.5(3)
<i>Z</i>	4	4	4
density (calcd)/g cm ⁻³	1.471	1.425	1.337
abs coeff/mm ⁻¹	0.940	0.824	0.867
<i>F</i> (000)	744	840	672
cryst size/mm ³	0.55 × 0.55 × 0.37	0.40 × 0.35 × 0.18	0.42 × 0.52 × 0.37
θ range for data collection/deg	2.17–29.99	1.58–30.00	2.77–30.00
index ranges	–21 ≤ <i>h</i> ≤ 21 0 ≤ <i>k</i> ≤ 16 0 ≤ <i>l</i> ≤ 12	–23 ≤ <i>h</i> ≤ 23 0 ≤ <i>k</i> ≤ 12 0 ≤ <i>l</i> ≤ 18	0 ≤ <i>h</i> ≤ 18 0 ≤ <i>k</i> ≤ 20 0 ≤ <i>l</i> ≤ 12
no. of reflns collected	4786	5518	2403
no. of ind reflns	4786	5518	2403
no. of reflns with <i>I</i> > 2σ(<i>I</i>)	3621	3903	1006
no. of data/restraints/params	4786/0/168	5517/0/298	2395/0/91
goodness-of-fit on <i>F</i> ²	1.052	1.034	1.023
final <i>R</i> indices [<i>I</i> > 2σ(<i>I</i>)] ^a	<i>R</i> 1 = 0.0356 w <i>R</i> 2 = 0.0835	<i>R</i> 1 = 0.0362 w <i>R</i> 2 = 0.0786	<i>R</i> 1 = 0.0654 w <i>R</i> 2 = 0.1427
<i>R</i> indices (all data) ^a	<i>R</i> 1 = 0.0605 w <i>R</i> 2 = 0.0940	<i>R</i> 1 = 0.0725 w <i>R</i> 2 = 0.0908	<i>R</i> 1 = 0.1959 w <i>R</i> 2 = 0.2056
largest diff peak and hole/e Å ⁻³	0.402 and –0.797	0.527 and –0.903	0.482 and –0.342

$$^a R1 = \sum ||F_o| - |F_c|| / \sum |F_o|. \quad wR2 = [\sum (w(F_o^2 - F_c^2)^2) / \sum (w(F_o^2)^2)]^{0.5}.$$

methyl hydrogens, 0.99 Å for methylene hydrogens, and 0.96 Å for Cp protons) and refined riding on the corresponding carbon atoms with isotropic thermal parameters ($U = 1.5U(\text{C}_{\text{methyl}})$, $1.2U(\text{C}_{\text{methylene}})$, and $1.2U(\text{C}_{\text{ring}})$). There is irresolvable disorder in the Cp ligand in **2**. The final *R* indices against the reflections with *I* > 2σ(*I*) were *R*1 = 0.0356 and w*R*2 = 0.0835 for **1a**, *R*1 = 0.0362 and w*R*2 = 0.0786 for **1b**, and *R*1 = 0.0654 and w*R*2 = 0.1427 for **2**. All calculations were performed on an Apple Macintosh computer.

Results and Discussion

Synthesis of Donor-Bridged Bis(silylene)molybdenum and -chromium Complexes. We have reported that photolysis of CpW(CO)₃Me in the presence of a hydrodisilane HSiMe₂SiMe₂Do afforded the donor-bridged bis(silylene)tungsten complexes CpW(CO)₂-(SiMe₂)₂Do (Do = OMe (**3a**), NEt₂ (**3b**)).¹⁷ In this work, the molybdenum and chromium analogues of the tungsten complexes were synthesized by a similar photolytic method. Photolysis of a C₆D₆ solution containing CpMo(CO)₃Me and an excess of HSiMe₂SiMe₂Do in a Pyrex NMR sample tube with a medium-pressure Hg lamp afforded bis(silylene)molybdenum complexes, **1a** and **1b**, together with small amounts of byproducts [CpMo(CO)₃]₂ and DoSiMe₂SiMe₂Do (eq 1).²⁸ Complexes **1a** and **1b** were isolated as pale yellow crystals in 33 and 44% yield, respectively, in large scale photolyses followed by crystallization. Bis(silylene)-chromium complex **2** was also synthesized by photolysis of a C₆D₆ solution containing CpCr(CO)₃Me and an excess of HSiMe₂SiMe₂Do. However, significant amounts of byproducts including [CpCr(CO)₃]₂, MeOSiMe₂SiMe₂OMe, and unidentified compounds were formed during the photolysis. Thus the isolated yield of **2** was rather low (12%) compared to those of the molybdenum and the tungsten complexes (50–54% yield for the



1a: M = Mo, Do = OMe

1b: M = Mo, Do = NEt₂

2: M = Cr, Do = OMe

tungsten complexes). The poor yield is mostly attributable to the photochemical and thermal instability of **2** in contrast with the tungsten and molybdenum analogues. Indeed, either photolysis or thermolysis (360 K) of a toluene solution of **2** gave a complex mixture of decomposition products, whereas no decomposition was observed for the molybdenum and tungsten complexes under the same experimental conditions. Complexes **1a**, **1b**, and **2** were fully characterized by spectroscopic methods, elemental analysis, and X-ray crystallography.

The ²⁹Si NMR signals of these complexes (**1a**, 117.6 ppm; **1b**, 80.5 ppm; **2**, 128.6 ppm) appear at significantly low field compared to those of known alkylsilylmolybdenum complexes (δ 20–69 ppm)²⁹ and are comparable to those of the known silylenemolybdenum (δ 111 ppm),²² alkyl- and arylsilylenechromium (δ 73–133 ppm),^{2,30,31} and bis(silylene)tungsten complexes (**3a**, 99.3 ppm; **3b**, 62.1 ppm).¹⁷ This indicates unsaturated character of the metal–silicon bonding in the bis(silylene) complexes.

The ²⁹Si NMR signals of the bis(silylene) complexes with group 6 metals shift to higher field on going from

(28) At the present time we are unable to offer a good explanation for the formation of DoSiMe₂SiMe₂Do.

(29) Koloski, T. S.; Pestana, D. C.; Carroll, P. J.; Berry, D. H. *Organometallics* **1994**, *13*, 489.

Cr to W in the group. A similar tendency has also been found for bis(silylene) complexes of group 8 metals, $\text{CpM}(\text{CO})\{\text{SiMe}_2\cdots\text{OMe}\cdots\{\text{SiMe}_2\}\}$ ($\text{M} = \text{Fe},^{14b} \text{Ru}^{16e}$), and some transition metal–group 14 element complexes.^{32–35} Lappert et al. found a similar trend in the ^{119}Sn NMR shift of tin–transition metal complexes and rationalized by a contribution of both paramagnetic and diamagnetic shielding effects.³⁶ On the basis of their interpretation, the higher field shifts observed for the bis(silylene) complexes with heavier metal atoms can be explained by a combination of the smaller paramagnetic contribution and larger diamagnetic contribution of neighboring atoms. The former is derived from larger values of the averaged excitation energy and higher polarizability of the heavier transition metal.³⁶ The latter is known to be proportional to Z/r , where Z is the atomic number of the contributing atom and r is its distance from the relevant nucleus.^{36,37}

The ^{29}Si NMR signals for methoxy-bridged bis(silylene) complexes, **1a** and **3a**, are shifted downfield compared to those of amino-bridged complexes, **1b** and **3b**, respectively.¹⁷ For monosubstituted silanes Me_3SiX , the ^{29}Si NMR signal shifts to lower field as the substituent X becomes more electronegative.³⁸ In other words, the ^{29}Si NMR signal shifts to lower field in the order $\text{X} = \text{F} > \text{Cl} > \text{Br} > \text{OMe} > \text{NMe}_2 > \text{Me}$. The low-field shift of the signals for the alkoxy-bridged complexes compared to that of the diethylamino-bridged complexes is consistent with this trend.

The ^1H NMR signals for the bridging methoxy group (δ 2.62 ppm for **1a** and 2.56 ppm for **2**) and diethylamino group (δ 2.40(br) and 0.67(br) ppm for **1b**) appear at higher field than those of the starting disilanes $\text{HSiMe}_2\text{-SiMe}_2\text{OMe}$ (δ 3.29 ppm) and $\text{HSiMe}_2\text{-SiMe}_2\text{NET}_2$ (δ 2.76 and 0.97 ppm), respectively. These high-field shifts of bridging group signals are characteristic for the donor-bridged bis(silylene) complexes.^{14,16–18}

The formation of the bis(silylene) complexes by the photolysis of a solution of $\text{CpM}(\text{CO})_3\text{Me}$ and $\text{HSiMe}_2\text{-SiMe}_2\text{Do}$ can be explained by the following mechanism, which is essentially the same as that proposed for the formation of bis(silylene)tungsten complexes:¹⁷ (i) photochemical elimination of a carbonyl group followed by oxidative addition of a Si–H bond of $\text{HSiMe}_2\text{-SiMe}_2\text{Do}$

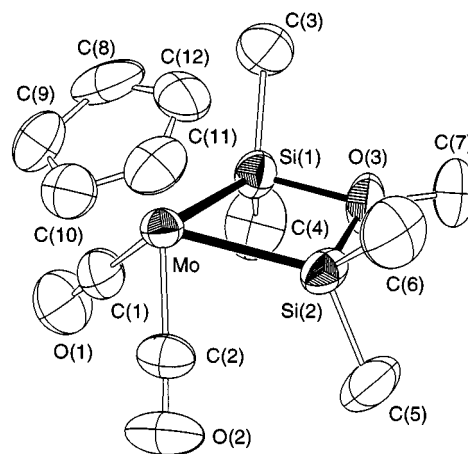


Figure 1. ORTEP drawing of **1a** with thermal ellipsoids shown at the 50% probability level.

Table 2. Selected Interatomic Distances [Å] and Angles [deg] for **1a**

Mo–Si(1)	2.4804(9)	Mo–Si(2)	2.4795(9)
Mo–C(1)	1.946(3)	Mo–C(2)	1.936(3)
Si(1)–O(3)	1.782(2)	Si(1)–C(4)	1.872(4)
Si(1)–C(5)	1.871(4)	Si(2)–O(3)	1.788(3)
Si(2)–C(6)	1.871(4)	Si(2)–C(7)	1.865(4)
O(1)–C(1)	1.156(4)	O(2)–C(2)	1.164(4)
O(3)–C(3)	1.446(4)	C(1)⋯C(4)	3.156(5)
O(1)⋯C(4)	3.283(5)	C(2)⋯C(5)	3.138(6)
O(2)⋯C(5)	3.267(5)	C(3)⋯C(7)	3.518(6)
C(4)⋯C(7)	3.437(6)	C(5)⋯C(7)	3.440(6)
C(6)⋯C(7)	3.558(6)		
C(2)–Mo–C(1)	79.04(14)	C(2)–Mo–Si(2)	73.59(11)
C(1)–Mo–Si(2)	111.75(10)	C(2)–Mo–Si(1)	115.64(10)
C(1)–Mo–Si(1)	75.30(10)	Si(2)–Mo–Si(1)	63.63(3)
C(5)–Si(1)–C(4)	106.3(2)	O(3)–Si(1)–Mo	100.22(8)
C(5)–Si(1)–Mo	125.7(2)	C(4)–Si(1)–Mo	116.51(13)
C(7)–Si(2)–C(6)	105.4(2)	O(3)–Si(2)–Mo	100.09(7)
C(7)–Si(2)–Mo	125.4(2)	C(6)–Si(2)–Mo	117.4(2)
C(3)–O(3)–Si(1)	131.9(3)	C(3)–O(3)–Si(2)	132.6(2)
Si(1)–O(3)–Si(2)	94.19(11)	O(1)–C(1)–Mo	177.8(3)
O(2)–C(2)–Mo	177.6(3)		

to give an 18-electron intermediate $\text{CpM}(\text{CO})_2(\text{H})(\text{Me})\text{-SiMe}_2\text{-SiMe}_2\text{Do}$ (**B**), (ii) reductive elimination of CH_4 from **B** affording a 16-electron disilanyl tungsten complex $\text{CpM}(\text{CO})_2\text{-SiMe}_2\text{-SiMe}_2\text{Do}$, and (iii) 1,2-silyl group migration of the silyl group SiMe_2Do to the metal center followed by cyclization to give the bis(silylene) complex $\text{CpM}(\text{CO})_2\{\text{SiMe}_2\cdots\text{Do}\cdots\{\text{SiMe}_2\}\}$.

Crystal Structures of 1a, 1b, and 2. Bis(silylene)molybdenum and -chromium complexes were characterized by X-ray crystal structure analysis (Figure 1 and Table 2 for **1a**, Figure 2 and Table 3 for **1b**, and Figure 3 and Table 4 for **2**). The complexes **1a** and **1b** are the first structurally characterized molybdenum complexes with a silylene ligand. The Mo–Si bonds (2.4804(9) and 2.4795(9) Å for **1a**; 2.4996(9) and 2.5008(9) Å for **1b**) are shorter than those of the known silylmolybdenum complexes (2.51–2.67 Å).^{29,39–41} The Cr–Si bond length of **2** (2.355(2) Å) is comparable to or shorter than those of the reported alkyl- and arylsilylenechromium complexes (2.36–2.53 Å).^{2,30} The short metal–silicon bond

(39) Berry, D. H.; Chey, J.; Zipin, H. S.; Carroll, P. J. *Polyhedron* **1991**, *10*, 1189.

(40) Malisch, W.; Lankat, R.; Fey, O.; Reising, J.; Schmitzer, S. J. *Chem. Soc., Chem. Commun.* **1995**, 1917.

(41) Chisholm, M. H.; Chiu, H.-T.; Folting, K.; Huffman, J. C. *Inorg. Chem.* **1984**, *23*, 4097.

(30) (a) Zybilla, C.; Müller, G. *Organometallics* **1988**, *7*, 1368. (b) Probst, R.; Leis, C.; Gampfer, S.; Herdtweck, E.; Zybilla, C.; Auner, N. *Angew. Chem., Int. Ed. Engl.* **1991**, *30*, 1132. (c) Handwerker, H.; Leis, C.; Probst, R.; Bissinger, P.; Grohmann, A.; Kiprof, P.; Herdtweck, E.; Blümel, J.; Auner, N.; Zybilla, C. *Organometallics* **1993**, *12*, 2162. (d) Handwerker, H.; Paul, M.; Blümel, J.; Zybilla, C. *Angew. Chem., Int. Ed. Engl.* **1993**, *32*, 1313. (e) Leis, C.; Wilkinson, D. L.; Handwerker, H.; Zybilla, C. *Organometallics* **1992**, *11*, 514. (f) Handwerker, H.; Paul, M.; Riede, J.; Zybilla, C. *J. Organomet. Chem.* **1993**, *459*, 151.

(31) (a) Corriu, R. J. P.; Lanneau, G. F.; Chauhan, B. P. S. *Organometallics* **1993**, *12*, 2001. (b) Corriu, R. J. P.; Chauhan, B. P. S.; Lanneau, G. F. *Organometallics* **1995**, *14*, 1646. (c) Corriu, R. J. P.; Chauhan, B. P. S.; Lanneau, G. F. *Organometallics* **1995**, *14*, 4014.

(32) Krentz, R.; Pomeroy, R. K. *Inorg. Chem.* **1985**, *24*, 2976.

(33) Li, S.; Johnson, D. L.; Grady, J. A.; Servis, K. L. *J. Organomet. Chem.* **1979**, *166*, 317.

(34) Kubicki, M. M.; Le Gall, J.-Y.; Kergoat, R.; Gomes de Lima, L. C. *Can. J. Chem.* **1987**, *65*, 1292.

(35) Pannell, K. H.; Rozell, J. M.; Cortez, S.; Kapoor, R. *Organometallics* **1990**, *9*, 1322.

(36) Harris, D. H.; Lappert, M. F.; Poland, J. S.; McFarlane, W. J. *Chem. Soc., Dalton Trans.* **1975**, 311.

(37) Jameson, C. J.; Mason, J. In *Multinuclear NMR*; Mason, J., Ed.; Plenum Press: New York, 1987; Chapter 3, p 51.

(38) Williams, E. A. In *The Chemistry of Organic Silicon Compounds*; Patai, S.; Rappoport, Z., Eds.; John Wiley & Sons: New York, 1989; Chapter 8, p 511.

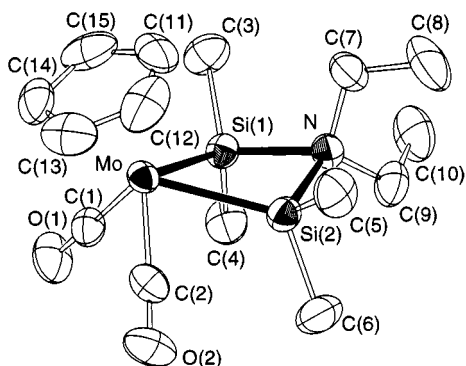


Figure 2. ORTEP drawing of **1b** with thermal ellipsoids shown at the 50% probability level.

Table 3. Selected Interatomic Distances [Å] and Angles [deg] for **1b**

Mo–Si(1)	2.4996(9)	Mo–Si(2)	2.5008(9)
Mo–C(1)	1.944(3)	Mo–C(2)	1.931(3)
Si(1)–C(3)	1.872(4)	Si(1)–C(4)	1.879(4)
Si(1)–N	1.933(2)	Si(2)–C(5)	1.876(4)
Si(2)–C(6)	1.874(4)	Si(2)–N	1.923(3)
N–C(7)	1.500(4)	N–C(9)	1.499(4)
C(1)–O(1)	1.162(4)	C(2)–O(2)	1.169(4)
C(7)–C(8)	1.526(6)	C(9)–C(10)	1.507(6)
C(1)···C(4)	3.109(5)	C(2)···C(6)	3.129(6)
O(1)···C(4)	3.264(5)	O(2)···C(6)	3.283(6)
C(3)···C(7)	3.160(6)	C(4)···C(9)	3.178(6)
C(5)···C(7)	3.290(7)	C(6)···C(9)	3.136(7)
C(2)–Mo–C(1)	81.33(13)	C(2)–Mo–Si(1)	113.71(10)
C(1)–Mo–Si(1)	74.01(10)	C(2)–Mo–Si(2)	72.54(10)
C(1)–Mo–Si(2)	111.69(9)	Si(1)–Mo–Si(2)	62.29(3)
C(3)–Si(1)–C(4)	104.5(2)	C(3)–Si(1)–Mo	115.86(14)
C(4)–Si(1)–Mo	121.8(2)	N–Si(1)–Mo	102.32(8)
C(6)–Si(2)–C(5)	103.4(2)	C(6)–Si(2)–Mo	122.6(2)
C(5)–Si(2)–Mo	114.9(2)	N–Si(2)–Mo	102.58(8)
C(9)–N–C(7)	110.3(3)	C(9)–N–Si(2)	119.0(2)
C(7)–N–Si(2)	112.1(2)	C(9)–N–Si(1)	118.7(2)
C(7)–N–Si(1)	110.1(2)	Si(2)–N–Si(1)	84.26(10)
O(1)–C(1)–Mo	176.7(3)	O(2)–C(2)–Mo	176.7(3)

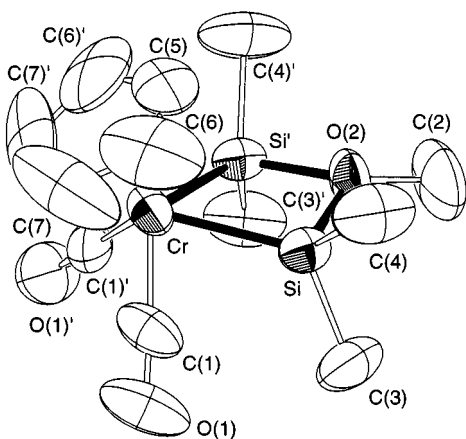


Figure 3. ORTEP drawing of **2** with thermal ellipsoids shown at the 50% probability level.

lengths indicate unsaturated character of the metal–silicon bonding, which is also supported by the low-field shift of ^{29}Si NMR signals (vide supra). The Si–O bonds in **1a** (1.782(2) and 1.788(3) Å) and **2** (1.788(3) Å) and Si–N bonds (1.933(2) and 1.923(3) Å) in **1b** are much longer than usual Si–O (1.63–1.65 Å) and Si–N single bonds (1.70–1.76 Å), respectively,⁴² and are comparable to those of the donor-bridged bis(silylene)iron, manganese, ruthenium, and tungsten complexes (1.93–1.96

Table 4. Selected Interatomic Distances [Å] and Angles [deg] for **2a**

Cr–Si	2.355(2)	Cr–C(1)	1.792(6)
Si–O(2)	1.788(3)	Si–C(3)	1.866(6)
Si–C(4)	1.875(6)	O(1)–C(1)	1.160(7)
O(2)–C(2)	1.464(10)	C(1)···C(3)	3.060(9)
O(1)···C(3)	3.205(8)	C(2)···C(3)	3.355(10)
C(2)···C(4)	3.591(10)		
C(1)'–Cr–C(1)	81.0(4)	C(1)'–Cr–Si	117.1(2)
C(1)–Cr–Si	75.6(2)	Si'–Cr–Si	65.79(8)
C(3)–Si–C(4)	105.7(3)	O(2)–Si–Cr	99.84(13)
C(3)–Si–Cr	123.3(2)	C(4)–Si–Cr	120.1(3)
C(2)–O(2)–Si	130.8(2)	Si–O(2)–Si'	91.3(2)
O(1)–C(1)–Cr	176.7(6)		

^a Symmetry transformation used to generate equivalent atoms: (') $x, -y + 1/2, z$.

Å for Si–N; 1.78–1.86 Å for Si–O).^{14,16a,b,e,17} The Si–O and Si–N bond lengths lie between that of the theoretically calculated value of $\text{H}_3\text{Si–OH}$ (1.65–1.67 Å)^{43,44} and that of $\text{H}_2\text{Si–OH}_2$ (2.10–2.13 Å)^{43,44} and between that of $\text{H}_3\text{Si–NH}_2$ (1.72 Å)⁴³ and that of $\text{H}_2\text{Si–NH}_3$ (2.04–2.09 Å),^{43,45} respectively. These structural data support that the Si–O and Si–N bonds are regarded as a hybrid of covalent bonding and dative bonding.

The four-membered ring defined by M, two Si, and the bridging atom is significantly bent to make the bridging atom and the Cp ring close. Dihedral angles between the Si–M–Si plane and the Si–X–Si (X = bridging atom) plane in **1a**, **1b**, and **2** are 166.5°, 152.4°, and 162.4°, respectively. Bending of the planes is attributable to the steric repulsion between the carbonyl ligands and methyl groups on the silicon atoms. The interatomic distances between the carbon atoms of carbonyl ligands and those of methyl groups (3.156(5) and 3.138(6) Å for **1a**, 3.109(5) and 3.129(6) Å for **1b**, and 3.060(9) Å for **2**) are much smaller than the sum of the van der Waals radii of methyl group and carbon atom (3.7 Å). The larger dihedral angle in the diethylamino-bridged bis(silylene)molybdenum complex **1b** than that in methoxy-bridged complex **1a** is due to the repulsion between the Si–Me and N–Et groups in **1b**. Interatomic distances between C(4)···C(9) (3.136(7) Å) and C(6)···C(9) (3.178(6) Å) in **1b** are significantly smaller than the sum of van der Waals radii of Me and the methylene group (4.0 Å).

Fluxional Behavior of Bis(silylene) Complexes. We have reported that the bis(silylene)tungsten complexes **3a** and **3b** show fluxional behavior in solution due to the rotation of silylene ligand.¹⁷ The molybdenum and chromium complexes also show similar fluxional behavior in solution. Figure 4 shows the variable-temperature ^1H NMR (VT ^1H NMR) spectra of **1b**. At 250 K, complex **1b** affords two singlets for the SiMe_2 groups and two quartets and two overlapping triplets for the NEt_2 group, which is consistent with the crystal structure shown in Figure 2. As the temperature is raised, these signals gradually broaden, coalesce, and finally become a singlet for the SiMe_2 groups and a set

(42) Sheldrick, W. S. In *The Chemistry of Organic Silicon Compounds*; Patai, S., Rappoport, Z., Eds.; John Wiley & Sons: New York, 1989; Chapter 3, p 227.

(43) Raghavachari, K.; Chandrasekhar, J.; Gordon, M. S.; Dykema, K. J. *J. Am. Chem. Soc.* **1984**, *106*, 5853.

(44) Su, S.; Gordon, M. S. *Chem. Phys. Lett.* **1993**, 204.

(45) Conlin, R. T.; Laakso, D.; Marshall, P. *Organometallics* **1994**, *13*, 838.

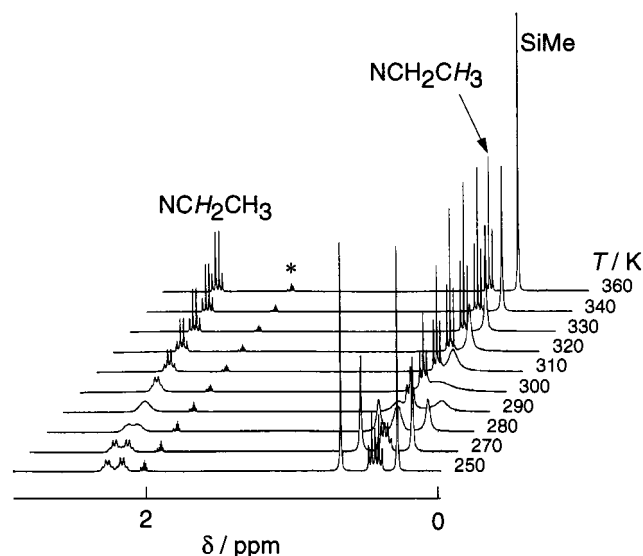


Figure 4. Variable-temperature ^1H NMR (300 MHz) spectra of **1b** measured in toluene- d_8 . *: $\text{C}_6\text{D}_5\text{CD}_2\text{H}$.

Table 5. Activation Parameters for the SiMe Exchange of **1a and **3a** and the SiMe and the NEt Exchange of **1b** and **3b****

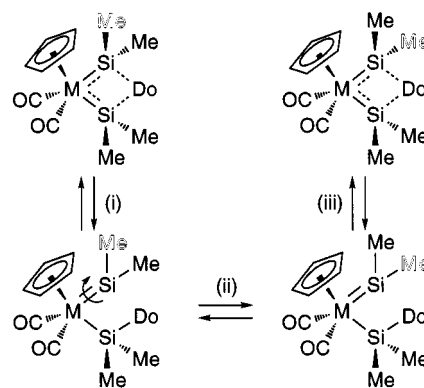
complex	probing signal	$\Delta H^\ddagger/\text{kJ mol}^{-1}$	$\Delta S^\ddagger/\text{J mol}^{-1} \text{K}^{-1}$
1a ^a	SiMe	61.0 (4.8)	11.6 (15.2)
1b ^a	SiMe	65.0 (3.3)	22.4 (5.1)
	methylene of NEt	49.1 (6.3)	-41.2 (21.6)
3a ^{a,c}	SiMe	70.2 (2.1)	39.9 (7.5)
3b ^{a,c}	SiMe	72.8 (3.3)	49.0 (10.5)
	methylene of NEt	63.4 (3.9)	10.6 (13.5)
3b ^{b,c}	SiMe	67.6 (1.5)	30.4 (5.1)
	methylene of NEt	67.7 (2.1)	24.9 (6.9)

^a Determined from VT ^1H NMR spectra. ^b Determined from VT $^{13}\text{C}\{^1\text{H}\}$ NMR spectra. ^c Reference 17.

of a quartet and a triplet for the NEt_2 group. The complexes **1a** and **2** also showed a similar spectral change for the Si–Me signals. However, in the case of complex **2**, severe decomposition occurred during the VT NMR measurement, which prevented further investigation. The activation parameters, $\Delta H^\ddagger/\text{kJ mol}^{-1}$ and $\Delta S^\ddagger/\text{J mol}^{-1} \text{K}^{-1}$, were determined by the complete band shape analysis⁴⁶ of the VT ^1H NMR spectra of the SiMe₂ signals of **1a** and that of the SiMe₂ signals and the methylene signals of the NEt_2 group of **1b** and are summarized in Table 5 along with those of the tungsten complexes. The activation parameters for the molybdenum complexes are comparable to those for the tungsten complexes.

We propose the following mechanism for the fluxional process (Scheme 2): (i) cleavage of a Si \cdots Do bond to form a base-free silyl(silylene) intermediate, (ii) rotation of the resulting M=Si double bond and, in the case of **1b**, rotation of the Si–N bond concomitant with inversion of amino group, and (iii) recombination of Do to the silylene ligand. This mechanism is essentially the same as those proposed previously for the fluxional behavior of silylene(germylene)- and bis(germylene)iron complexes,²³ bis(silylene)tungsten complexes **3a** and **3b**,¹⁷

Scheme 2



and bis(silylene)ruthenium complexes.¹⁸ The rate-determining step would be the cleavage of the Si \cdots Do bond (step i) since the rotation barriers around the M=Si bond in silylene complexes $(\text{OC})_5\text{M}=\text{SiHR}$ (M = Cr, Mo; R = H, OH) have been calculated to be very small (0.46–1.5 kJ mol⁻¹) due to fairly weak π -bonding interaction between metal and silylene ligand.^{47–49}

We previously reported that the HOMO of the bis(silylene)iron complex is made up of the π back-bonding interaction between the metal fragment and the SiR₂· \cdots Do \cdots SiR₂ fragment and has an antibonding character on Si \cdots Do bonding.⁵⁰ The electron-rich group 6 metal fragment weakens the Si \cdots Do bond by the strong back-donation to the σ^* orbital of Si \cdots Do bonds.⁵¹ This facilitates formation of the base-free silyl(silylene) intermediate and also stabilizes the intermediate by π back-donation to the empty p orbital of the silylene ligand. In addition to the electronic factor, steric factors also are important for the fluxionality of bis(silylene) complexes **1a**, **1b**, and **2** as well as **3a** and **3b**. As described, there is severe steric repulsion between carbonyl ligands and methyl groups in the silylene ligands, which bends the four-membered ring defined by M, two Si, and the bridging atoms significantly to make the bridging atom and the Cp ring close. Cleavage of the Si \cdots O bond to give the base-free silyl(silylene) intermediate releases the steric strain.

Acknowledgment. This work was supported by Grants-in-Aid for Scientific Research (No. 09440223 and 10132203) from the Ministry of Education, Science, Sports and Culture of Japan.

Supporting Information Available: Tables of crystal data and structural refinement, atomic coordinates and equivalent isotropic displacement parameters of non-hydrogen atoms, full bond lengths and angles, anisotropic displacement parameters, and hydrogen coordinates and isotropic displacement parameters for **1a**, **1b**, and **2**. This material is available free of charge via the Internet at <http://pubs.acs.org>.

OM990201F

(47) Nakatsuji, H.; Ushio, J.; Yonezawa, T. *J. Organomet. Chem.* **1983**, 258, C1.

(48) Márquez, A.; Sanz, J. F. d. *J. Am. Chem. Soc.* **1992**, 114, 2903.

(49) Jacobsen, H.; Ziegler, T. *Inorg. Chem.* **1996**, 35, 775.

(50) Ueno, K.; Tobita, H.; Ogino, H. *J. Organomet. Chem.* **1992**, 430, 93.

(51) Crabtree, R. H. In *The Organometallic Chemistry of the Transition Metals*, 2nd ed.; John Wiley & Sons: New York, 1994; p 42.

(46) (a) Stephenson, D. S.; Binsch, G. *DNMR5*; Program QCPE365; Quantum Chemistry Program Exchange, Indiana University: Bloomington, IN, 1978. (b) LeMaster, C. B.; LeMaster, C. L.; True, N. S. *DNMR5 (IBM-PC version)*; Program QCMP059; Quantum Chemistry Program Exchange, Indiana University: Bloomington, IN, 1988.